Available online at www.sciencedirect.com
SCIENCE DIRECT
Tectonophysics 420 (2006) 301–316
TECTONOPHYSICS
www.elsevier.com/locate/tecto

Lessons from a joint interpretation of vibroseis wide-angle and near-vertical reflection data in the northeastern Yilgarn, Western Australia

T. Fomin *, B.R. Goleby [1]

Predictive Mineral Discovery Cooperative Research Centre, c/-Geoscience Australia, GPO Box 378, Canberra, ACT, 2601, Australia
ANSIR, c/-Research School of Earth Sciences, Australian National University, Canberra, ACT, 0200, Australia

Received 31 March 2005; received in revised form 30 September 2005; accepted 4 January 2006
Available online 3 April 2006

Abstract

A wide-angle reflection seismic experiment was carried out in the Eastern Goldfields granite–greenstone terrane of the Archaean Yilgarn Craton during 2001. This was the first time in Australia that wide-angle data were collected using a vibrator source and with a high density of observations. Unlike other wide-angle surveys carried out in other parts of the world, our survey used both a smaller number of sweeps, and shorter sweeps. We recorded three sweeps (each with its own frequency range) at each vibration point. The experiment demonstrated that the sum of three 12 s sweeps using 3 large vibrators provides enough energy to record signal at offsets up to up to 60–70 km. A comparison of individual shot gathers from near-vertical data and receiver gathers from wide-angle data demonstrated higher reflectivity in near-vertical data. This may be due to differences in the frequency bands of the recording equipment. The after stack section obtained from dense wide-angle data is different from that obtained from conventional near-vertical reflection data. The conventional reflection section provides higher quality image of the crust compared to the wide-angle section. This could be explained by the low-fold in wide-angle data and differences in the acquisition and processing methodology. The wide-angle survey, which was coincident with a regional vibroseis seismic reflection transect, was focused on the Leonora–Laverton region. The survey was designed to supplement the deep seismic reflection studies with velocity information. This also created an opportunity to compare velocity model derived from wide-angle reflection seismic data with a structural image obtained from the deep common mid-point seismic reflection data, and thus refine our geological understanding of the area. A high velocity body reaching a maximum thickness of 2 km was identified exclusively from the seismic velocity model derived from wide-angle study. This body is interpreted as mafic rocks within the Archaean Granite–Greenstone Belt. The joint interpretation also shows that structural boundaries do not always follow lithological boundaries in our study area. The combination of wide-angle reflection and near-vertical reflection data has facilitated a more complete geological interpretation of the seismic data.

Keywords: Wide-angle reflection technique; Near-vertical reflection technique; Vibroseis source; Velocity modelling; Crustal reflectivity; Archaen Yilgarn Craton

1. Introduction

The vibroseis seismic reflection technique has been widely used for imaging the Earth's crust since the late 1970s and early 1980s (Mooney and Brocher, 1987).

* Corresponding author. Tel.: +61 2 6249 9725; fax: +61 2 6249 9772.
E-mail address: tanya.fomin@ga.gov.au (T. Fomin).
[1] Tel.: +61 2 6249 9725; fax: +61 2 6249 9772.

0040-1951/$ - see front matter © 2006 Elsevier B.V. All rights reserved.
doi:10.1016/j.tecto.2006.01.015

Vibroseis sources for wide-angle experiments were first used in tests and pilot studies in the early 1980s (Yushin, 1982; Liu et al., 1986; Dammotte et al., 1987), and coincident with reflection seismic surveys since the middle 1980s (DEKORP RESEARCH GROUP, 1990; Heikkinen et al., 2004; Luschen et al., 2004). The results

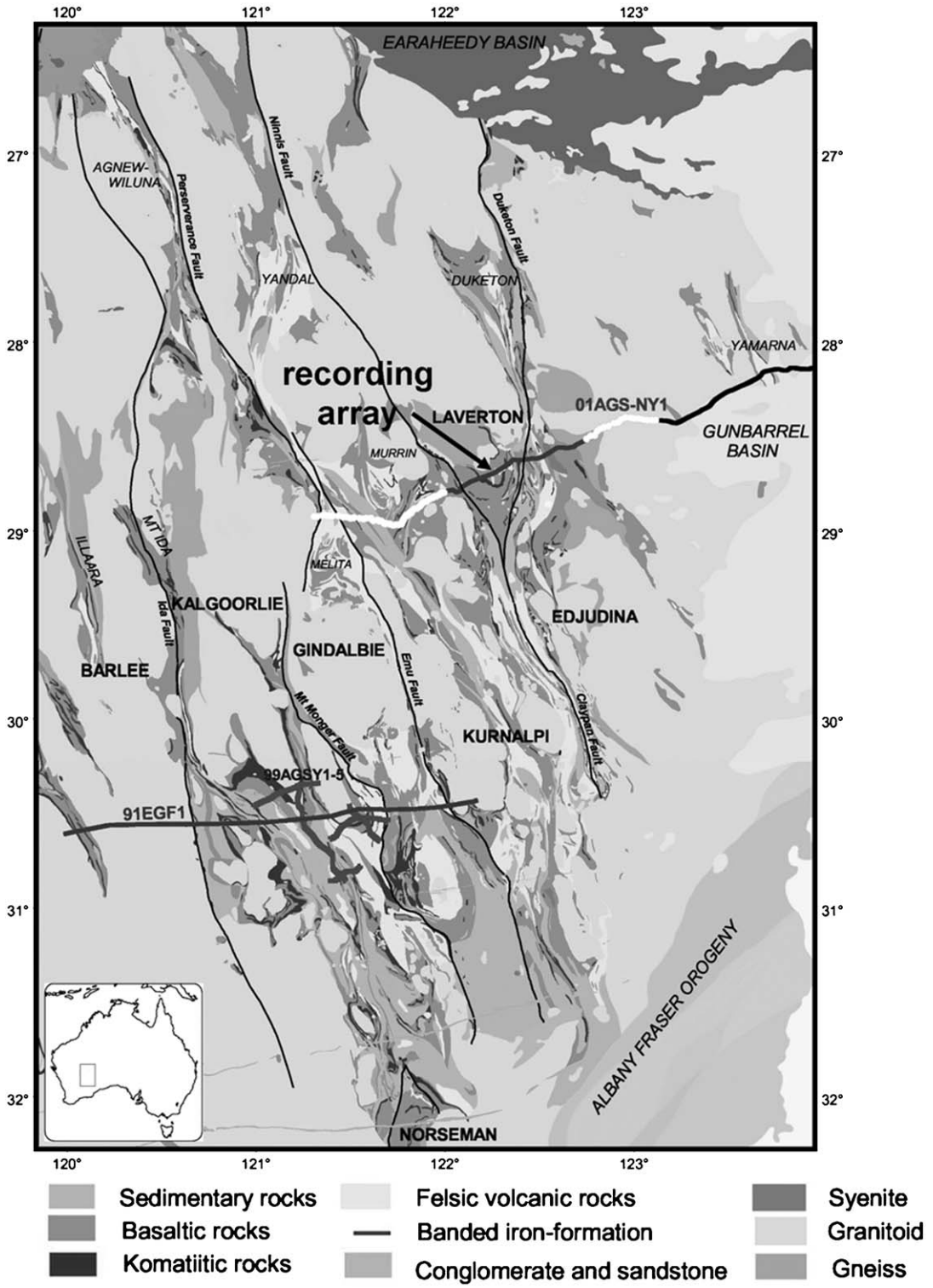

of comparison of deep reflection and wide-angle techniques using explosive source, vibroseis, or combination of two sources, have been discussed in a number of papers (Berry and Mair, 1980; Braile and Chiang, 1986; Mooney and Brocher, 1987; Brocher and Hart, 1991; Berzin et al., 2002; Bleibinhaus et al., 2003). These concluded that reflection and wide-angle techniques image different features of the crust as a result of differences in the frequency contents, acquisition and/or processing methodologies of the two techniques.

In Australia, low-fold deep seismic reflection profiling with explosive sources has been successfully used for many years to image the deep crust (Mathur et al., 1977; Moss and Mathur, 1986; Moss and Dooley, 1988; Goleby et al., 1993; Drummond et al., 1998; Gibson et al., 1998). Geoscience Australia, in collaboration with State Geological Surveys and the Predictive Mineral Discovery Co-operative Research Centre (pmd*CRC) has been collecting deep seismic reflection data with Vibroseis source since 1999.

The Northeastern Yilgarn Seismic Survey in Western Australia was undertaken in 2001 to improve our understanding of the 3D crustal architecture of the granite–greenstone terranes of the Eastern Goldfields Province. The province hosts several world-class gold deposits. Seismic studies of the area include a refraction survey (Mathur, 1974), and explosive and vibroseis reflection profiling (Drummond and Goleby, 1993; Goleby et al., 2000, 2002) (Fig. 1). Despite these studies and significant exploration and scientific interest, the crustal architecture of this mineral province is still poorly understood (Dentith et al., 2000).

The 2001 survey was carried out as a part of an integrated study that included several seismic techniques: deep common mid-point seismic reflection profiling (CMP), wide-angle reflection, and broadband receiver function experiments. Preliminary results of the wide-angle experiment were published by Fomin et al. (2003) and Fomin (2005). The CMP reflection work provided new information on crustal reflectivity, and was published by Goleby et al. (2003) and Goleby and Blewett (2005). Results from the receiver function experiment were discussed in Reading et al. (2003a,b) and Reading et al. (2003a,b).

The purpose of this paper is to present the results from the vibroseis wide-angle experiment, and compare this data with the coincident deep CMP reflection data collected simultaneously from the same vibroseis source.

The 432-km long seismic reflection transect crosses the Eastern Goldfields Province of the Archaean Yilgarn Craton. The craton is comprised mainly of granite and greenstone rocks (Myers, 1997; Drummond et al., 2000). The survey represents the first time wide-angle data collected in Australia using a vibroseis source. The wide-angle line focussed on the Leonora–Laverton tectonic zone that includes mostly greenstones (Fig. 1). One of the aims of the survey was to determinate if the quality and resolution of wide-angle data will be sufficient to distinguish greenstones and granites on the basis of velocity differences between these rock types (Christensen and Mooney, 1995), and to map the boundary between these rock units.

Most of the existing wide-angle surveys with vibrator sources carried out in other parts of the world were designed specifically for collecting wide-angle data, or used reflection source parameters with long sweeps (Liu et al., 1986; Dammotte et al., 1987; DEKORP RESEARCH GROUP, 1990; Davidson and Braile, 1999; TRANSALP Working Group, 2001; Yliniemi et al., 2004). Such designs are targeted at producing energy level comparable with high-energy explosive sources, and include long sweeps of 20–32 s length and sum 8 to 50 sweeps per vibration point from at least four heavy Vibrator trucks.

The Eastern Goldfields wide-angle experiment used the same parameters we normally used for near-vertical reflection acquisition. In this respect, the survey differs from other wide-angle experiments. We used only three relatively short sweeps, each 12 s long. The acquisition parameters of a vibroseis near-vertical reflection survey were selected from our experience of previous reflection surveys in the Yilgarn region.

Initially, it was unclear if the acquisition parameters designed for the reflection survey would suit the wide-angle reflection experiment, and if the seismic energy produced by the vibrators would be sufficient to record

Fig. 1. Location of wide-angle and near-vertical seismic surveys on the simplified geological map of the NE Yilgarn Craton (after Groenewald et al., 2003). 174-km long wide-angle seismic line comprises 64-km long fixed recording array (black segment of the line high-lighted by an arrow) and extension vibration points on both ends of the recording array (75 km extension to the west and 35 km extension to the east, shown as white segments of the line). Coincident near-vertical data were recorded along the whole 174 km of wide-angle line. Reflection line with only near-vertical recording continues further east from the eastern end of wide-angle line (black segment shows part of the 01AGS-NY1 line within map limits). Early explosive (91EGF1) and vibroseis (99AGSY1-5) reflection profiles are shown as black lines.

signal at large offsets. Therefore, the first task of the wide-angle survey was to test if it was possible to collect high spatial density wide-angle data at large offsets (60 km and more) using acquisition parameters of a typical Australian reflection survey with a vibrator source. We also wanted to supplement the deep seismic reflection data with velocity information (mainly for the upper crust), and to better interpret the petrology of the Leonora–Laverton Region. Finally, we wanted to compare the seismic images of the crust constructed from near-vertical and wide-angle data, and velocity model derived from wide-angle data interpretation and interpretation of the conventional reflection section.

2. Design of the wide-angle experiment, data collection, and data processing

The 174 km long wide-angle line included the 64 km-long fixed recording array (Fig. 1). The line covered the area of main geological interest, and was extended by additional vibration points to the west by 75 km and to the east by 35 km (extensions are shown as white lines in Fig. 1). As a result, offsets were in the range of 95 to 139 km. We decided to extend the wide-angle line by additional vibration points despite results from previous surveys around the world in which vibroseis signals were recorded up to maximum offsets of 60–80 km. For example, in the joint wide-angle survey of ECORS and DECORP, signal from vibrator sources was detected up to 82 km, with 48 sweeps at every vibration point — each 20 s long (Dammotte et al., 1987); in the Rhenish Massif by DEKORP and BELCORP signals from a vibrator source (10–70 sweeps, each 20 s long, per vibration point) were collected at distance up to 60 km (DEKORP RESEARCH GROUP, 1990). In the more recent TRANSALP and FARE wide-angle experiments signals (8–10 sweeps at every vibration point, each 28–30 s long) are detectable to 80 km distance from a source (TRANSALP Working Group, 2002; Kukkonen et al., 2004).

In our experiment, 120 short period instruments were deployed at ~500 m interval along a 64-km long fixed array. The recording and source parameters are presented in Table 1. These parameters were selected from experience of previous vibroseis reflection surveys in the Yilgarn region and on the basis of an extended experimental program carried out prior to commencing of the reflection survey. The parameters are optimised for vibroseis reflection and were chosen without considering the wide-angle survey. Therefore, wide-angle data were collected passively utilising acquisition parameters of reflection survey.

The short period portable recorders were designed by the Research School of Earth Sciences at the Australian National University (ANU). A detailed description of the acquisition parameters, logistics of the survey, and details of the wide-angle data processing were given in Fomin et al. (2003).

Data were processed and displayed using several separate software packages such as:

- a non-commercial software developed at the ANU for displaying field data and converting raw data into SEGY format;

Table 1
Seismic acquisition parameters

Wide-angle survey recording parameters:		Energy source parameters:	
Type of recorders	Short period portable	Vibrator type	IVI Hemi (60,000 lb each)
Number of recorders	120	Number of vibrators	3
Spacing interval	~500 m	Vibrator points interval	80 m
Sample rate	10 ms	Source move-up	15 m
Type of seismometer	1 Hz, one-component	Sweep length	12 s
Listening time	Continuous	Sweep type	Linear
		Sweep mode	Varisweep
		Sweep frequency	7–56, 12–80, 8–72 Hz
		Number of vibration points (collected during wide-angle survey)	2137
Reflection survey recording parameters (ARAM recording system):			
Sample rate			2 ms
Group interval			40 m (12 seismometers in-line)
Listening time			18 s

- DISCO/FOCUS — a commercial package for the processing of conventional reflection data for producing receiver gathers and after-stack sections;
- PETROSYS — commercial package for the digitising of major seismic events to input travel times to a modelling package;

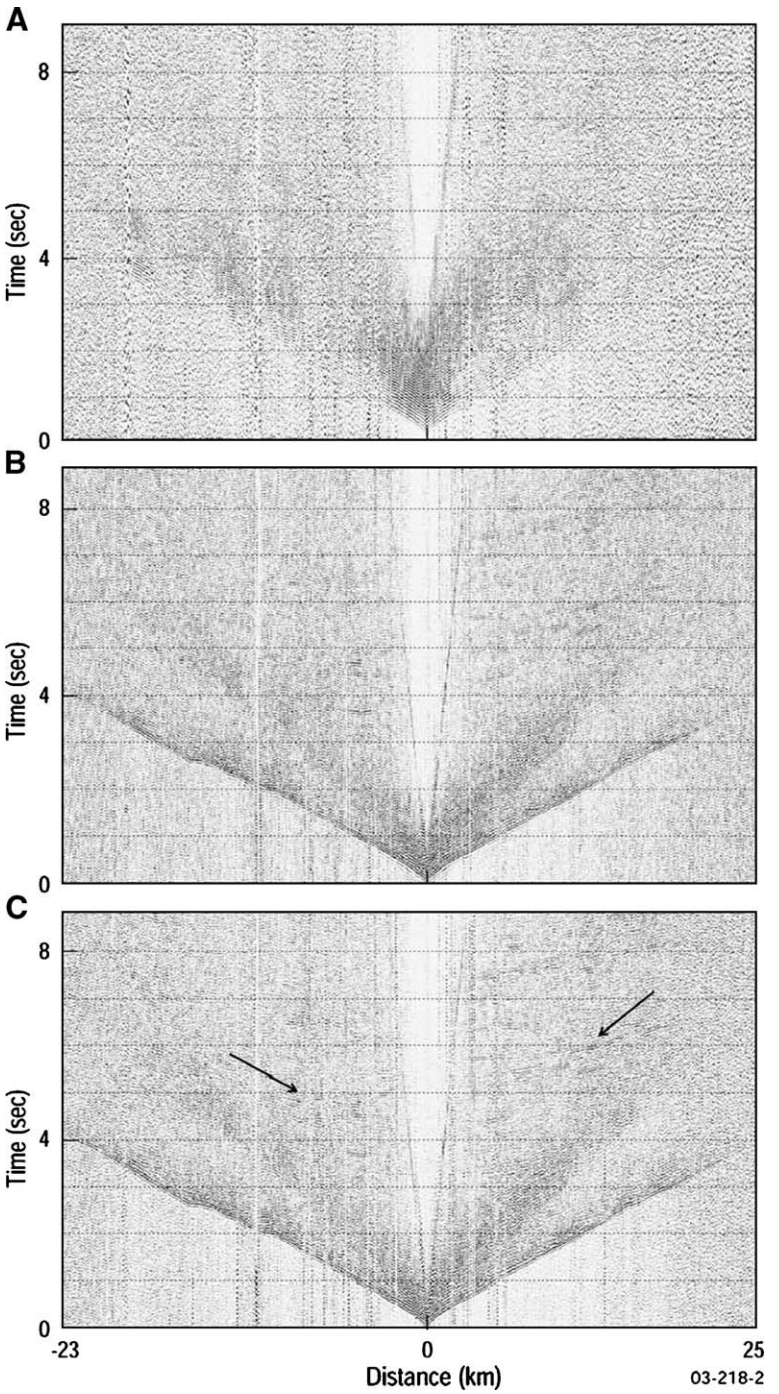

Fig. 2. Example of a common receiver gather for station 3473 (fragment) at different stages of processing. Non-correlated receiver gather (A), receiver gather after cross-correlation with reference sweep (B) and vertical stack of three cross-correlated common receiver gathers (C). Only 12–80 Hz sweep shown in (A) and (B), sweeps with other frequency bands do not result in visibly different receiver gathers. 7–56, 12–80 and 8–72 Hz sweeps vertically stacked in (C). Arrows highlight some wide-angle reflections that were used to design velocity model of the upper crust.

- SIGMA modelling software — 2-D seismic travel time modelling software based on Zelt and Smith's algorithm (Zelt and Smith, 1992) to develop seismic velocity model;
- GOCAD — commercial 3-D modelling package to convert the velocity model obtained in SIGMA for comparison with the interpretation of reflection seismic data.

Wide-angle data were extracted from continuos recordings based on the GPS vibration times taken from the near-vertical reflection recording system. For every vibration point, one minute of data starting from vibration time was extracted and converted to SEGY format. From this step onwards we processed SEGY data in the DISCO/FOCUS software package. Data were arranged into common receiver gathers with 80 m interval between traces and cross-correlated with appropriate reference sweeps characterised in Table 1. The resulting individual impulse-type traces were vertically stacked on the assumption that every three sweeps belong to the same vibration point. In practice, there was a 15 m offset between individual vibration points, which were ignored due to its negligible effect.

A summary of the processing sequence of wide-angle data is as follows:

- Extraction of one minute long traces, based on GPS timings of vibration starts for every vibration;
- Conversion of extracted data to SEG-Y format;
- Arranging traces into common receiver gathers;
- Generation of synthetic reference sweeps and cross-correlation of individual traces in common receiver gathers with appropriate sweep;
- Vertical stacking of all three sweeps generated at the same vibration point;
- Application of a minimum-phase band-pass filter (5/10–25/30 Hz);
- Reduction of data using a velocity of 8 km/s;
- Balancing of amplitudes prior to final display.

More than 600,000 individual vibrations were collected during 2 weeks of survey; 118 common receiver gathers were produced with an average of 2000 traces per gather. Data were recovered from 65 stations; data from 15 recorders were lost because of technical failure. Data from another 40 stations were collected only for very close offsets (1 to 5 km) — probably because of the low gain setting for these recorders which were originally designed for the recording of teleseismic events. As a result, effective station spacing along the line varied from 500 to 3000 m. Data quality was generally very good: first arrivals were easily identified, as well as changes of refracted waves of different nature becoming first arrivals, and subsequent wide-angle reflections. Typically, high amplitude arrivals were observed at up to 50 km offsets and in some gathers up to 60–70 km. Wide-angle reflections at ~5.5, 7.0, 9.5 and 12.0 two-way time at 0 km offset can be tracked to 20–50 km offsets and are believed to originate from boundaries in the lower crust. Fig. 2 illustrates the different stages of processing of the common receiver gather. A set of three non-correlated receivers gathers (one for each sweep) was produced for every recording station (Fig. 2A). Each of these gathers was cross-correlated with a synthetic reference sweep (Fig. 2B). After the cross-correlation was performed for every individual sweep, and the three sweeps were vertically stacked at each vibration point, first arrivals and reflections become quite clear (Fig. 2C). Reflections arriving later than 4 s two-way time originate below 12 km depth. Travel time variation of the first arrivals is a distinct feature of this data set which translates into a model with lateral velocity variation.

3. Velocity modelling and interpretation of the results

Travel times from 65 stations were used to develop the final seismic velocity model for the upper crust (Fig. 3). Fig. 3 is a compilation of all travel times picked from common receiver gathers, including those of first arrivals and deep crustal reflections that were used for developing a velocity model.

The process of developing the final velocity model included several stages:

- design of a starting model based purely on wave field analysis of wide-angle data (assigning of refracted arrivals to particular boundaries in the crust, estimation of apparent velocity characterising every layer of the model at different locations along the profile, determination of the nature of later arrivals, analysis of reversed and overlapping travel time curves to localise velocity anomalies in the crust);
- development of a first-pass velocity model using a limited travel time sub-set from only 5 stations with an average spacing of 16 km; extension vibration points on both sides of 64 km long recording array to develop a velocity model extending beyond the recording array to cover the whole 174 km long line even for this limited sub-set (Fomin et al., 2003);
- development of a second-pass model based on data from 20 stations with an average spacing of ~3 km;

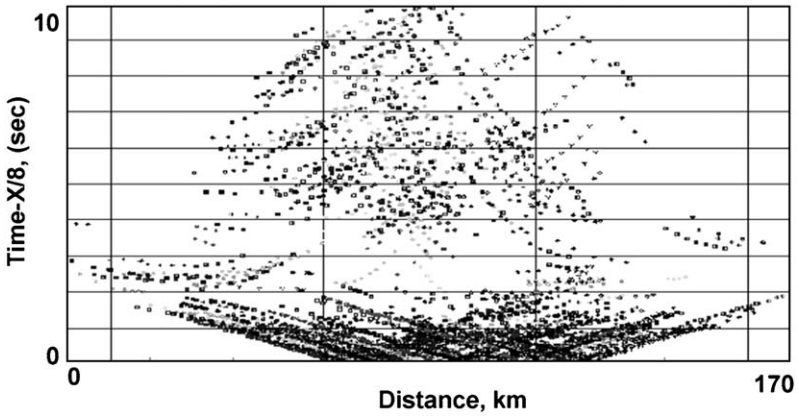

Fig. 3. Compilation of all travel times for major seismic events, picked from common receiver gathers for 65 recording stations. Time scale reduced by 8 km/s velocity.

- development of the final model based on all data from 65 stations with recorder spacing varying between 0.5 and 3.0 km.

The product of each stage was used as a starting model for the next stage. Travel time modelling software, based on the ray-tracing algorithm of Zelt and Smith (Zelt and Smith, 1992; Zelt et al., 2003) was used. A ray tracing diagram showing ray paths of first arrivals and later crustal reflections is presented in Fig. 4. For convenience of modelling, and because of the very dense geometry of observations, we split the dataset into three sub-sets, each containing a selection of 20 different stations at average spacing of ~3 km. At the final stage the model was adjusted to fit travel times from the whole dataset. The final overall RMS deviation of calculated travel times from experimental picks is ~70 ms, which was achieved through iterative ray-tracing.

The final upper crustal velocity model shows a broad range of seismic velocity variation in the upper 14 km of the crust (Fig. 5). The model consists of four layers and a high-velocity body localised at the bottom of layer 2 in the western part of the line. The first layer is a thin upper layer with velocity gradually increasing

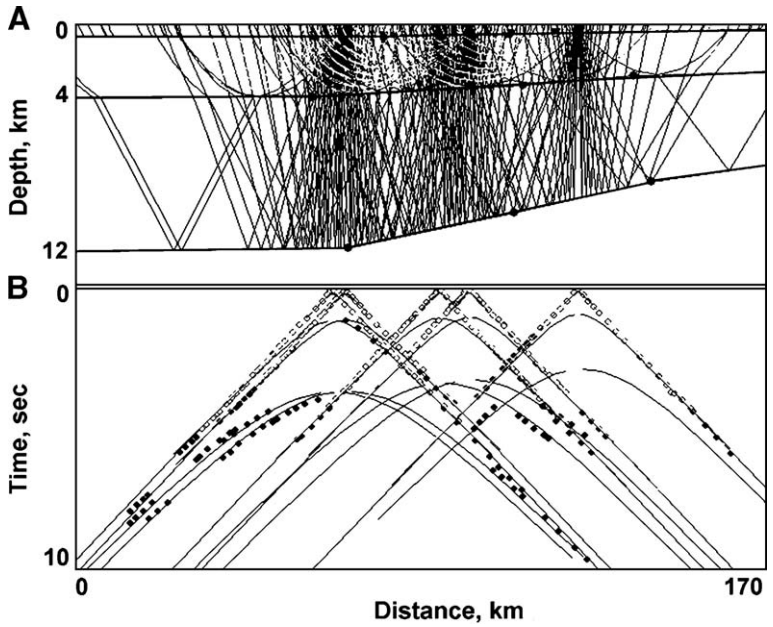

Fig. 4. Ray-tracing diagram for selected 5 stations (A) and corresponding travel time plot (B), showing observed (squares) and calculated (lines) travel times. 5 out of 65 stations selected to improve resolution of the figure. Open symbols — refractions, closed symbols — reflections.

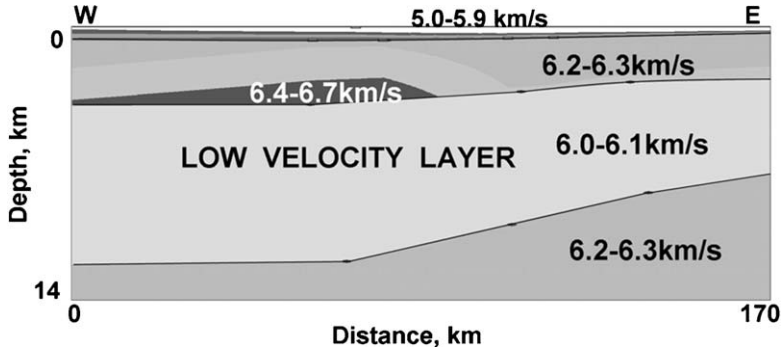

Fig. 5. Final velocity model of the upper crust in the Leonora–Laverton tectonic zone based on refractions and wide-angle reflections from 65 recording stations. Ranges of velocity variation in each layer correspond to velocity values at the top and bottom of each layer.

from 5.0 to 5.9 km/s. The second layer is ~3 km thick, and it has velocity increasing with depth from 6.2 to 6.3 km/s. A high velocity body (6.4–6.7 km/s) reaching a maximum thickness of 2 km is interpreted as mafic rocks within the Archaean Granite–Greenstone Belt and it is restricted to the western part of the line with its top at ~3 km depth. The third layer is 4 to 8 km thick, has a relatively low velocity (6.0–6.1 km/s) typical for granite–gneissic composition. Its top is at ~12 km depth in the western part of the line and shallows to ~7 km in the east. The fourth layer has the same velocity as layer 2. It was diagnosed by refractions penetrating it and recorded as first arrivals. These waves are parallel to refractions from layer 2 and are delayed, indicating the presence of a low velocity layer 3 in between layers 2 and 4.

The travel times for deep crustal reflections (Fig. 3) were used to develop a velocity model for the middle/lower crust. The match between computed and observed travel times of the lower crustal reflections does not exceed 100 ms for the velocity model of the middle/lower crust illustrated in Fig. 6. Velocity in the middle/lower crust in this model increases from 6.4 to 6.5 km/s and leads to Moho depth of 33–34 km along the line. However, by changing velocity in the middle/lower crust and shifting reflectors respectively up or

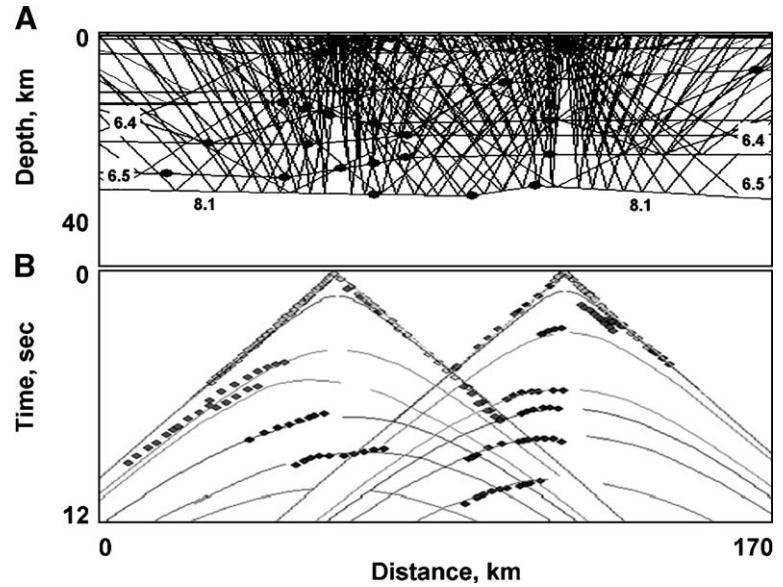

Fig. 6. One of the possible models of the lower crust (A) and corresponding ray-tracing diagram (B) for two stations based on first arrivals and wide-angle reflections. Black dots in A show locations where depth to boundaries was defined in the model. Velocity in the middle/lower crust increases from 6.4 to 6.5 km/s, upper mantle velocity — 8.1 km/s. This particular velocity in the middle/lower crust leads to Moho depth of 33–34 km along the line. In the travel time plot (B), squares and lines show observed and calculated travel times respectively.

down from the original positions, we can achieve similar matches for velocity models within several hundred m/s deviations from the model of Fig. 6. Therefore, the velocity model of the middle/lower crust, which is based on wide-angle reflections only, is less constrained than the upper crustal one presented in Fig. 5, and the lower crustal refractions and supercritical reflections from the Moho are required to better constrain it. The signal from the vibroseis source was too weak to record such refractions at larger offsets. By using more sweeps and longer sweeps (e.g., 8–10 sweeps each 28–30 s long) other

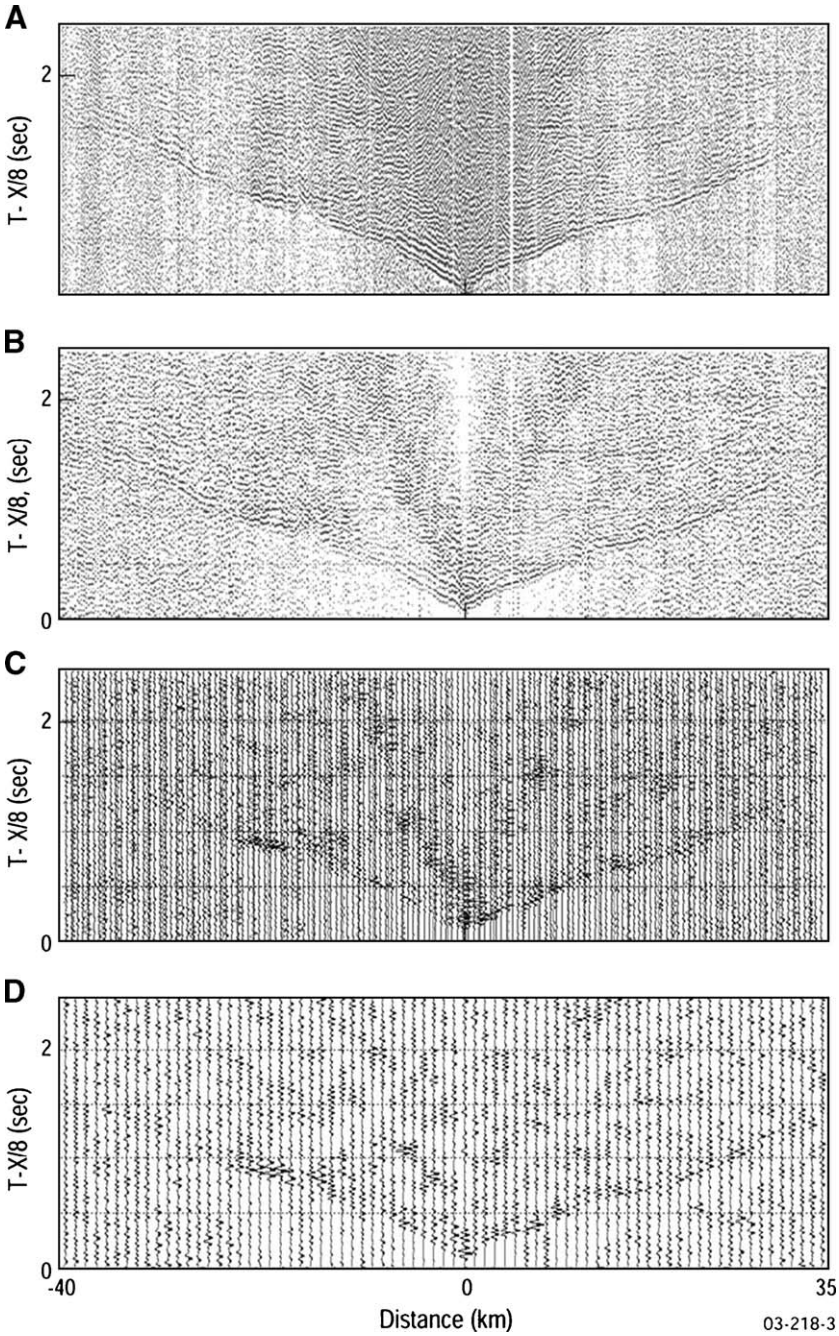

Fig. 7. Wide-angle data in common receiver domain at variable degree of decimation: original 80 m vibration point interval recorded in the field (A); 240 m interval, or every 4th trace preserved (B); 480 m interval, or every 7th trace preserved (C); 960 m interval, or every 13th trace preserved (D).

researchers were able to record first arrivals from the lower crust to a maximum of 80 km offset (TRANSALP Working Group, 2002; Yliniemi et al., 2004). However, even these sweeps are not sufficient to map lower crust all the way down to the Moho in typical continental environment where crustal thickness reaches 40 km or more. We conclude that higher energy explosive sources are needed to collect data to support modelling of the middle/lower crust.

4. Optimum shot and recorder intervals

In this section we discuss the significance of shot and recorder intervals for reliable phase correlation of events with a view that such correlation has to result in accurate representation of identified events by their travel times only.

The major challenge in processing and modelling the wide-angle data was to manage a huge data set collected during the survey. Two key survey parameters: shot and recorder intervals were considered to minimise the amount of data required to develop a velocity model without sacrificing the quality of final result.

Several common receiver gathers were used to choose an optimal vibration point interval for further surveys. Fig. 7 illustrates how dramatically the reliability of correlation of seismic phases changes in the process of traces decimation. First and later arrivals can be picked without losing phase correlation of events when a maximum 240 m interval between shots is preserved (Fig. 7B). This means that only every 4th trace from the original data set illustrated in Fig. 8A is preserved. It should be noted that when intervals between traces is increased to 480 or 960 m (Fig. 7C, D) wide-angle reflections are not identifiable and correlation of first arrivals does not allow the identification of arrivals necessary for development of a reliable velocity model of the upper crust: individual phases could be lost and arrivals misidentified.

In developing the final velocity model (Fig. 5) we started with 5 stations at average recorder intervals of 20 km and moved progressively to 65 stations at recorder intervals of 0.5 to 3 km. For our dataset, increasing the recorder density spacing from 3 to 1 km did not change the velocity model significantly; while increasing recorder density from a spacing of 20 to 3 km did change the velocity model. For example, the high velocity body appears to be located shallower by as much as 1.5–2.0 km as a 6 times denser ray coverage becomes available.

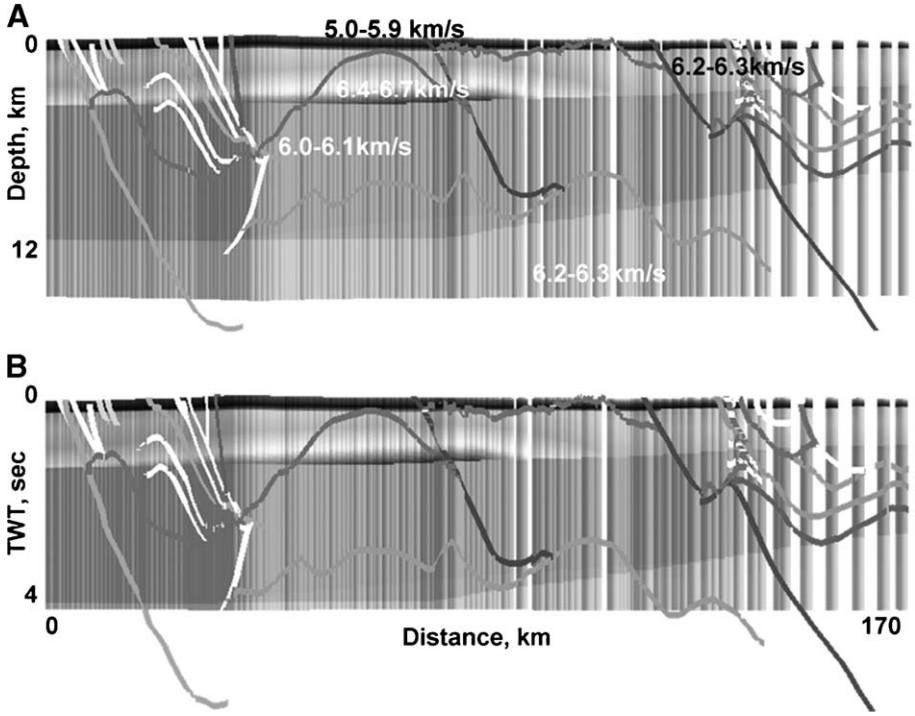

Fig. 8. Seismic velocity model of Fig. 5 with superimposed simplified interpretation of reflection seismic data in depth (A) and two-way time scale (B). Display created using 3-D modelling package GOCAD. Reflection interpretation of Goleby et al. (2003) shown as lines. Vertical stripes are due limitation of extrapolation function in GOCAD. Vertical exaggeration 1:3.5.

There is no obvious answer to the question of optimal recorder density because the degree of detail required to obtain geologically meaningful interpretation may be hard to predict a priori. Our preference, for the type of data analysis that we used, is a 3–10 km interval between recorders — depending on the geology of the area. Looking retrospectively, such dense observations provided sufficient data to build a velocity model of the upper crust that was accurate enough to satisfy the requirements of geological interpretation.

It also has to be taken into consideration that shot and receiver intervals are important for other potential uses of our data, e.g. waveform processing. If waveform processing is going to be carried out, then care has to be taken so that the data are not spatially aliased. Within a common receiver gather, spatial aliasing occurs when the shot spatial sampling interval (ΔX) is greater than

$$\Delta X = V_{\min}/2f_{\max},$$

where $V_{\min}$ is the slowest velocity in the wave field, and $f_{\max}$ is the maximum frequency (Brocher et al., 1982). At 10 Hz and apparent velocity of 6.0 km/s, ΔX can be 300 m. For surface waves having a $V_{\min}$ of 1.0 km/s, at 10 Hz, $\Delta X = 50$ m. Therefore, it would be advisable to keep all our original traces (80 m spacing) for the analysis.

5. Comparison of wide-angle and conventional reflection data

A comparison of wide-angle and conventional reflection data sets includes two aspects: comparison of the velocity model derived from wide-angle and seismic interpretation obtained from reflection section (Fig. 8); and the comparison of receiver and shot gathers (Fig. 9), and stack sections from both data sets (Fig. 10).

The wide-angle data set complements the reflection dataset by providing more robust velocity information. The velocity model derived from wide-angle data was used to depth-convert the reflection interpretation. The GOCAD® 3-D modelling package was used for depth-to-time conversion of velocity model developed in SIGMA and time-to-depth conversion of reflection

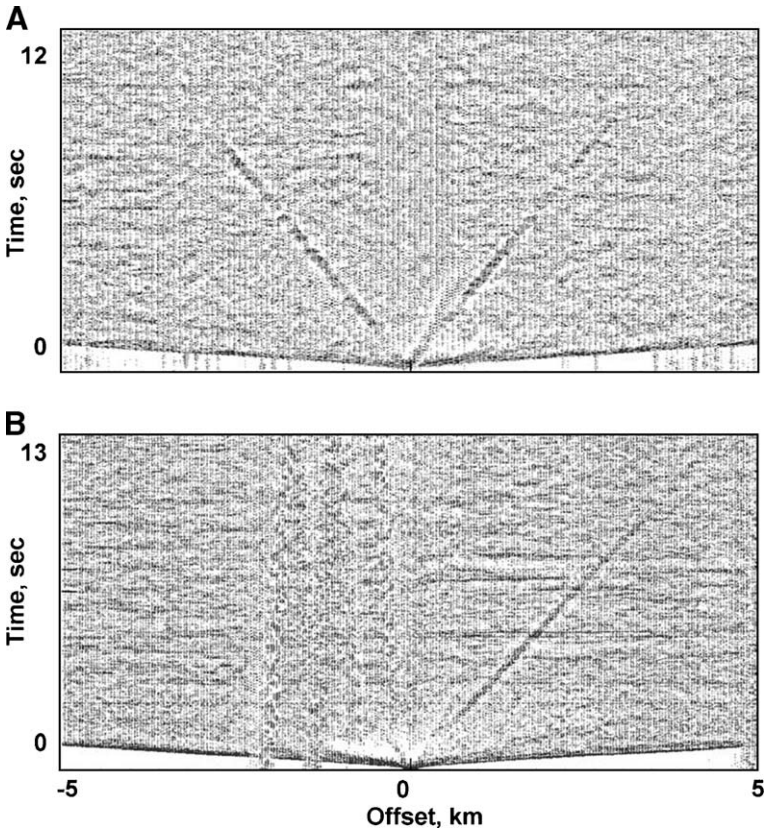

Fig. 9. Comparison of pre-stack data from wide-angle (common receiver gather, A) and near-vertical reflection (common shot gather, B) surveys. Wide-angle offsets were limited to 5 km in (A), and all available near-vertical offsets shown in (B). Equal trace spacing of 80 m in both (A) and (B).

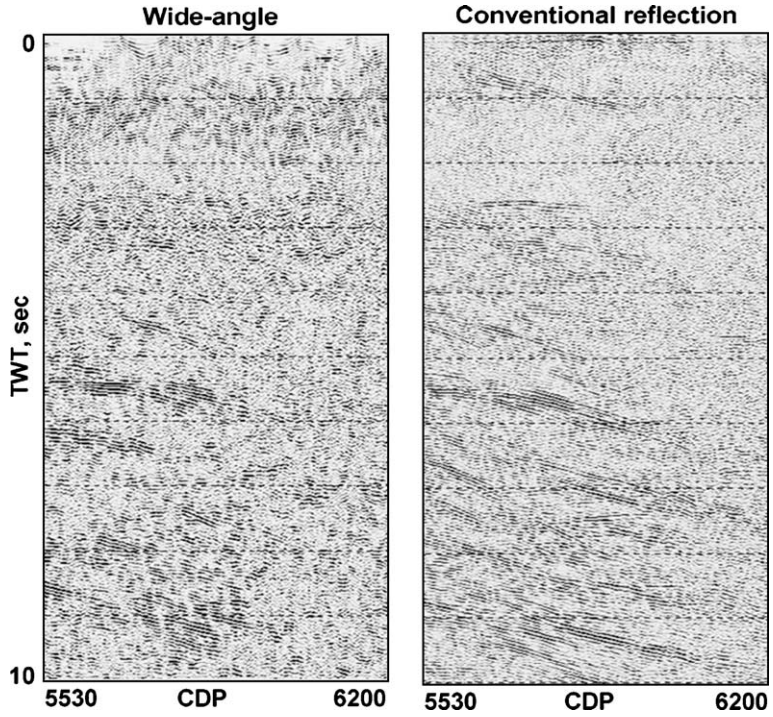

Fig. 10. Fragments of after-stack seismic sections resulting from 3–4 fold data (left panel) and 60-fold near-vertical reflection data (right panel). CDP interval is 20 m. Both fragments are 13.4 km long.

interpretation shown in Fig. 8. There is no significant difference between the two-way time and depth scale images because of small lateral variations of average velocity along the line. This is because significant lateral variation of seismic velocity in individual layers in our final model (Fig. 5) is balanced along vertical profiles through the crust (e.g., a high-velocity body is underlain by a thicker layer of lower velocities).

The reflection data image structures within the upper crust quite well, but fail to detect long wavelength seismic velocity stratification. There is no obvious correlation between interpreted seismic reflection horizons and velocity boundaries. The high-velocity body (6.4–6.7 km/s) imaged in the wide-angle data appears to be relatively transparent in the reflection seismic image, and it is located partly under an anti-formal structure interpreted as a low-angle shear zone (Goleby et al., 2003). This zone is relatively non-reflective compared to the eastern and western flanks of the line where steeply dipping reflective horizons are observed. Such relationship between reflectivity and velocity model suggests that the velocity model is probably controlled more by lithology changes in the crust rather than by structure. Metamorphism associated with the formation of the greenstone belt is likely to have caused rather smooth long wavelength velocity variation superimposed on top of finer scale structural changes in the crust imaged by the reflection data.

Another example of mismatches between structural and lithological boundaries is a recent study by Drummond et al. (2004) of a detachment fault zone in the Eastern Goldfields Province. This regional subhorizontal detachment zone is characterised as a thick shear zone of multiple layers, which are linked by faults. In some places it forms the base of greenstones, while in other places it is located below it. This detachment zone does not consistently follow a lithological boundary and it is possibly controlled by contrasts in rheology.

Due to a high density of wide-angle data with ~500 m intervals between recorders and 80 m shot spacing, we were able to produce a CDP stack and compare the after-stack section with a conventional reflection section along the same line. A comparison of the pre-stack wide-angle and near vertical data shows that there are fewer reflections in the wide-angle data set, in the similar range of offsets (Fig. 9), possibly due to the lower frequency range (10 ms sample interval, 25 Hz anti-alias filter) in wide-angle recording. The nominal fold determined by the spacing of recorders and shots, and by the number of channels was as high as 9. But given the data losses during the survey, the maximum achievable fold

was 3 to 4. It is essential to supply data from all recorders to the stacking process to achieve as high fold as possible, but including data with high noise levels did not improve the quality of the stack section. Common receiver gathers with high noise levels were excluded from the stacking process, thus improving the quality of wide-angle stack section. Forty common receiver gathers were used to produce the final wide-angle stack section.

For producing stack section from wide-angle data we used conventional processing similar to that used for near-vertical data (Fig. 10). Refraction static corrections were calculated for reflection data using travel times picked from the first arrivals and velocity of bedrock (Jones et al., 2003). The same refraction static corrections were applied to wide-angle data. Stacking velocity functions used for normal moveout (NMO) correction were chosen on the basis of stacking velocity analysis of reflection data and velocity model derived from wide-angle data. The integrated velocity model was then simplified and used for NMO correction prior to stack. A summary of the processing scheme used to stack the wide-angle data is as follows:

- definition of line geometry according to receiver and shot locations;
- sorting data into common receiver gathers;
- refraction static correction (same as for reflection data);
- application of a minimum-phase band-pass filter (5/10–25/30 Hz);
- NMO correction using velocity functions from reflection data tested on common receiver gathers;
- editing noisy traces from receiver gathers and excluding receiver gathers with high level of noise;
- sorting in CDP gathers (only CDPs within 1000 m radius were included into CDP bin);
- application of NMO;
- stacking of data;
- signal enhancement for display (algorithm based on enhancing of coherent seismic signals within specified range of dips);
- amplitude balancing for display of final section.

In general, the wide-angle stack section appears to be less reflective compared to the reflection section. A comparison of the after-stack wide-angle and near-vertical sections for a small part of the line is presented in Fig. 10. Despite the fact that the same source was used to record both data sets, ray paths were different. Therefore, the spectra of the propagating energy were different, and, as a result, interference of seismic waves at finely stratified intervals of the section also has been different. This difference may have led to the enhancement of certain elements of the acoustic structure in one data set and to their attenuation in the other data set. This contrast probably explains observable differences between the two after-stack images, which are high-lighted in Fig. 10. These differences may also be due to technical reasons such as: a lower frequency cut-off in wide-angle data compared to near-vertical data (7 vs. 80 Hz); lower fold in wide-angle data; and the different normal move-out correction required for larger offsets. A sampling rate of at least 4 ms and a 0.5–1.5 km recorder interval are required to achieve better resolution of after-stack wide-angle sections and to provide a more sensible comparison with the conventional reflection section.

It also has to be taken into account that the wide-angle receiver was a point receiver, while the near-vertical incidence data used a receiver array to attenuate surface and air wave energy (12 geophones were grouped on 40 m base). The effect of this grouping is clearly visible in Fig. 9 which shows far superior suppression of low velocity energy for the vertical incidence data than for the wide-angle survey. We cannot completely rule out that under-suppressed surface and air wave energy is still present in the after-stack wide-angle images in some form, and therefore it may also be responsible for differences between the near-vertical and wide-angle images compared in Fig. 9.

6. Conclusions

This work presents the first Australian wide-angle data set collected using a vibrator source. Unlike other wide-angle surveys carried out in other parts of the world, our survey used a smaller number of sweeps and shorter sweeps. We recorded three sweeps (each had its own frequency range) at each vibration point. The experiment demonstrated that the sum of three 12 s long sweeps produced by 3 large vibrators provides enough energy to record signal up to 60–70 km offsets. Wide-angle reflections at ~5.5, 7.0, 9.5 and 12.0 two-way time at 0 km offset were also recorded, and they can be tracked to 20–50 km offsets and are believed to originate from boundaries in the lower crust.

The final upper crustal velocity model shows a broad range of seismic velocity variation in the upper 14 km of the crust. The model consists of four layers and a high-velocity body localised at the bottom of layer 2 in the western part of the line. A high velocity body reaching a maximum thickness of 2 km, and interpreted as mafic rocks within the Archaean Granite–Greenstone Belt, was identified from the seismic velocity model derived

from wide-angle study only. It does not appear in near-vertical reflection data. The velocity model of the middle/lower crust, based on wide-angle reflections only, is less constrained than the upper crustal model. Lower crustal refractions and super-critical reflections from the Moho are required to better constrain it. A higher energy explosive source is needed to collect data to support modelling of the middle/lower crust.

Our analysis of the shot and recorder intervals required in wide-angle work leads to a conclusion that first and later arrivals can be picked without losing the phase correlation of events when a maximum 240 m interval between shots is preserved. This means that only every 4th trace from the original data set has to be preserved. However, if waveform processing is going to be carried out, then care has to be taken so that the data are not spatially aliased. The spatial sampling interval required to achieve this can be as low as 50 m. Therefore, in this case it would be advisable to keep all the original traces (80 m spacing) for the analysis.

The reflection data image structures within the upper crust quite well, but fail to detect long wavelength seismic velocity stratification. Consistent with earlier presented results from other parts of the world, we do not observe obvious correlation between interpreted seismic reflection horizons and velocity boundaries in the crystalline crust of our study area.

A comparison of pre-stack wide-angle and near vertical data shows that there are fewer reflections in the wide-angle data set, for a similar range of offsets. The after-stack section resulting from the wide-angle data also appears to be less reflective compared to the after-stack section constructed from near-vertical data. Apart from technical reasons (e.g., lower frequency range in wide-angle recording) this may be due to the way seismic signal interacts with geological media. Despite the fact that the same source was used to record both data sets, ray paths were different. This means that the spectra of the propagating energy were different, and, as a result, the interference of seismic waves at finely stratified intervals of the section must also have been different. This difference may have led to enhancement of certain elements of the acoustic structure in one data set and to their attenuation in the other data set. This could explain the observable differences between the two after-stack images.

Overall, our experiment has demonstrated the effectiveness of a vibroseis source for the recording of wide-angle data simultaneously with reflection survey, and a more comprehensive geological interpretation has become possible using a combination of wide-angle and reflection seismic techniques.

Acknowledgements

The authors are grateful to Australian National Seismic Imaging Resources (ANSIR) facility for providing wide-angle recording equipment to collect the data, with special thanks to Tim Barton, David Johnstone, Leonie Jones, and Alan Crawford for supporting this project. We thank the ANU staff for participation in the field work and providing the software for data processing. We also thank Barry Drummond for inspiring this work. We thank the members of Yilgarn Y2 Project Team for providing the seismic interpretation of reflection data with special thanks to Malcolm Nicoll for producing velocity model image in GOCAD® software package. We thank Barry Drummond and Alexey Goncharov for reviewing earlier versions of the manuscript. This paper has benefited from useful comments from Guest Editor D. Snyder and reviewer T. Brocher, and an anonymous reviewer.

The authors publish with the permission of the Chief Executive Officer of Geoscience Australia and the Chief Executive Officer of Predictive Mineral Discovery CRC. Geoscience Australia catalogue number for this paper is 61891.

References

Berry, M.J., Mair, J.A., 1980. Structure of the continental crust: a reconciliation of seismic reflection and refraction studies. Spec. Pap. Geol. Assoc. Can. 20, 195–213.

Berzin, R.G, Yurov, Yu.G., Pavlevkova, N.I., 2002. CDP and DSS Data along the Uchta-Kem Profile (the Baltic Shield). Tectonophysics 355, 187–200.

Bleibinhaus, F., Gebrande, H., TRANSALP Working Group, 2003. 3D simultaneous reflection and refraction seismic tomography based on SIMULPS13Q with application to the TRANSALP wide-angle data. Seismix 2003, the 10th International Symposium on Deep Seismic profiling of the Continents and their Margins, Programme and Abstracts, poster, 6–10 January 2003, Huka Village Conference Centre, Taupo, New Zealand.

Braile, L.W., Chiang, C.S., 1986. The continental Mohorovicic discontinuity: result from near-vertical and wide-angle seismic reflection studies. In: Barazangi, M., Brown, L. (Eds.), Reflection Seismology: A Global Perspective. Geodyn. Ser., vol 13. AGU, Washington, D.C., pp. 257–272.

Brocher, T.M., Hart, P.E., 1991. Comparison of vibroseis and explosive source methods for deep crustal seismic reflection profiling in the Basin and Range province. J. Geophys. Res. 96 (B11), 18,197–18,213.

Brocher, T.M., Kempner, W.L., Gettrust, J.F., 1982. A comparison of synthetic p-tau sections for proposed models of two ophiolites. J. Geophys. Res. 87, 9355–9364.

Christensen, N.I., Mooney, W.D., 1995. Seismic velocity structure and composition of the continental crust: a global review. J. Geophys. Res. 100 (B6), 9761–9788.

Dammotte, B., Fuchs, K., Luschen, E., Wenzel, F., Schlich, R., Toreilles, G., 1987. Wide-angle vibroseis test across the Rhine Graben. Geophys. J. R. Astron. Soc. 89, 313–318.

Davidson, M.E., Braile, L.W., 1999. Vibroseis recording techniques and data reduction from the Jemez tomography experiment. Bull. Seismol. Soc. Am. 89 (5), 1352–1365.

DEKORP RESEARCH GROUP, represented by Flueh E.R., Klaeschen D. and Meissner R., 1990. Wide-angle Vibroseis Data from the Western Rhenish Massif. Tectonophysics 173, 83–93.

Dentith, M.C., Dent, V.F., Drummond, B.J., 2000. Deep crustal structure in the Southwestern Yilgarn Craton, Western Australia. Tectonophysics 325, 227–255.

Drummond, B.J., Goleby, B.R., 1993. Seismic reflection images of the major ore-controlling structures in the Eastern Goldfields Province, Western Australia. Explor. Geophys. 24, 473–478.

Drummond, B.J., Goleby, B.R.G., Goncharov, A.G., Wyborn, L.A.I., Collins, C.D.N., MacCready, T., 1998. Crustal-scale structures in the Proterozoic Mount Isa Inlier of North Australia: their seismic response and influence on mineralisation. Tectonophysics 288, 43–56.

Drummond, B.J., Goleby, B.R., Swager, C.P., 2000. Crustal signature of Late Archaean tectonic episodes in the Yilgarn Craton, Western Australia. Tectonophysics 329, 193–221.

Drummond, B.J., Hobbs, B.E., Goleby, B.R., 2004. The role of crustal fluids in the tectonic evolution of the Eastern Goldfields Province of the Archaean Yilgarn Craton, Western Australia. Earth Planets Space 56, 1163–1169.

Fomin, T., 2005. Wide-angle refraction studies. In: Blewett, R.S., Hitchman, A.P. (Eds.), Final Report, 3D Geological Models of the Eastern Yilgarn Craton, Y2 project September 2001 to December 2004, Predictive Mineral Discovery*CRC, pp. 90–103.

Fomin, T., Crawford, A., Johnstone, D., 2003. A wide-angle reflection experiment with Vibroseis sources as part of a multidisciplinary seismic study of the Leonora–Laverton Tectonic Zone, Northeastern Yilgarn Craton. Explor. Geophys. 34, 147–150.

Gibson, G.M., Drummond, B.J., Fomin, T., Owen, A.J, Maidment, D., Gibson, D.L., Peljo, M., Wake-Dyster, K.D., 1998. Re-evaluation of crustal structure of the Broken Hill Inlier through structural mapping and seismic profiling. Australian Geological Survey Organisation, Record 1998/11, vol. 55.

Goleby, B.R., Blewett, R.S., 2005. Seismic reflection studies of the northeastern Yilgarn Craton. In: Blewett, R.S., Hitchman, A.P. (Eds.), Final Report, 3D Geological Models of the Eastern Yilgarn Craton, Y2 Project September 2001 to December 2004, Predictive mineral discovery*CRC, pp. 90–99.

Goleby, B.R., Rattenbury, M.S., Swager, C.P., Drummond, B.J., Williams, P.R., Sheraton, J.E., Heinrich, C.A., 1993. Archaean crustal structure from seismic reflection profiling, Eastern Goldfields, Western Australia. In: Williams, P.R., Haldane, J.A. (Eds.), Kalgoorlie'93 — An International Conference on Crustal Evolution, Metallogeny, and Exploration of the Eastern GoldfieldsAustralian Geological Survey Organisation, Record 1993/54.

Goleby, B.R., Bell, B., Korsch, R.J., Sorjonen-Ward, P., Groenewald, P.B., Wyche, S., Bateman, R., Fomin, T., Witt, W., Walshe, J., Drummond, B.J., Owen, A.J., 2000. Crustal structure and fluid flow in the Eastern Goldfields, Western Australia. Australian Geological Survey Organisation, Record, 2000/34, p. 109.

Goleby, B.R., Korsch, R.J., Fomin, T., Bell, B., Nicoll, M.G., Drummond, B.J., Owen, A.J., 2002. A preliminary 3D geological model of the Kalgoorlie region, Yilgarn Craton, Western Australia, based on deep seismic reflection and potential field data. Aust. J. Earth Sci. 49, 917–934.

Goleby, B.R., Blewett, R., Groenewald, B., Cassidy, K., Champion, D., Korsch, R.J., Whitaker, A., Jones, L.E.A., Bell, B., Carlson, G., 2003. Seismic interpretation of the northeastern Yilgarn Craton seismic data. In: Goleby, B.R., Blewett, R.S., Groenewald, P.B., Cassidy, K.F., Champion, D.C., Jones, L.E.A., Korsch, R.J., Shevchenko, S., Apak, S.N. (Eds.), The 2001 Northeastern Yilgarn Deep Seismic Reflection Survey. Geoscience Australia, Record, 2003/28, pp. 85–112.

Groenewald, B., Morris, P.A., Champion, D., 2003. Geology of the eastern Goldfields and an overview of tectonic models. In: Goleby, B.R., Blewett, R.S., Groenewald, P.B., Cassidy, K.F., Champion, D.C., Jones, L.E.A., Korsch, R.J., Shevchenko, S., Apak, S.N. (Eds.), The 2001 Northeastern Yilgarn Deep Seismic Reflection Survey. Geoscience Australia, Record, 2003/28, pp. 63–84.

Heikkinen, P., Kukkonen, I.T., P.A., Ekdahl, E., Hjelt, S.-E., Koria, A., Lantinen, R., Vuollo, J., Yliniemi, J., Berzin, R., FIRE WORKING GROUP, 2004. FIRE-4 transect in Lapland, northern Finland: crustal reflection images and comparison with POLAR velocity data. Seismix 2004, the 11th International Symposium on Deep Structure of the Continents and their Margins, Programme and Abstracts, 26 September–1 October 2004, Centre des congres, Mont-Tremblant, Quebec, Canada.

Jones, L.E.A., Goleby, B.R., Barton, T.J., 2003. Seismic processing — 2001 Northeastern Yilgarn seismic reflection survey (L154). In: Goleby, B.R., Blewett, R.S., Groenewald, P.B., Cassidy, K.F., Champion, D.C., Jones, L.E.A., Korsch, R.J., Shevchenko, S., Apak, S.N. (Eds.), The 2001 Northeastern Yilgarn Deep Seismic Reflection Survey. Geoscience Australia, Geoscience Australia, Record, 2003/28, pp. 27–48.

Kukkonen, I.T., Heikkinen, P., Ekdahl, E., Hjelt, S.-E., Koria, A., Lantinen, R., Yliniemi, J., Berzin, R., FIRE WORKING GROUP, 2004. FIRE transects: new images of the crust in the Fennoscandian Shield. Seismix 2004, the 11th International Symposium on Deep Structure of the Continents and their Margins, Programme and Abstracts, 26 September–1 October 2004, Centre des congres, Mont-Tremblant, Quebec, Canada.

Liu, C.-S., Zhu, T., Farmer, H., Brown, L., 1986. An expanding spread experiment during COCORP's field operation in Utah. In: Barazangi, M., Brown, L. (Eds.), Reflection Seismology: A global perspective. Geodyn. Ser., vol 13. AGU, Washington, D.C., pp. 237–246.

Luschen, E., Lammerer, B., Gebrande, H., Millahn, K., Nicolich, R., TRANSALP Working Group, 2004. Orogenic structure of the Eastern Alps, Europe, from TRANSALP deep seismic reflection profiling. Tectonophysics 388, 85–102.

Mathur, S.P., 1974. Crustal structure in the Southwestern Australia from seismic and gravity data. Tectonophysics 24, 151–182.

Mathur, S.P., Moss, F.J., Branson, C., 1977. Seismic and Gravity Investigations along the Geotraverse, Western Australia, 1969. BMR Bull. 191 (63 pp.).

Mooney, W.D., Brocher, T.M., 1987. Coincident seismic reflection/refraction studies of the continental lithosphere: a global review. Rev. Geophys. 25, 723–742.

Moss, F.J., Dooley, J.C., 1988. Deep crustal reflection recordings in Australia 1957–1973 — I. Data acquisition and presentation. Geophys. J. 93, 229–237.

Moss, F.J., Mathur, S.P., 1986. A review of continental reflection profiling in Australia. In: Barazangi, M., Brown, L. (Eds.), Reflection Seismology: A Global Perspective. Geodyn. Ser., vol 13. AGU, Washington, D.C., pp. 67–76.

Myers, J.S., 1997. Preface: Archaean geology of the Eastern Goldfields of Western Australia — regional overview. Precambrian Res. 83, 1–10.

Reading, A.M., Kennett, B.L.N., Dentith, M.C., 2003a. Lithospheric structure of the Pilbara Craton, Capricorn Orogen and northern

Yilgarn Craton, Western Australia, from teleseismic receiver functions. Aust. J. Earth Sci. 50, 439–445.

Reading, A.M., Kennett, B.L.N., Dentith, M.C., 2003b. Seismic structure of the Yilgarn Craton, Western Australia. Aust. J. Earth Sci. 50, 427–438.

TRANSALP Working Group, 2001. European Orogenic Processes Research Transects the Eastern Alps. Eos, Trans, American Geophysical Union, vol. 82, 453 and 460–461.

TRANSALP Working Group, 2002. First deep seismic reflection images of the Eastern Alps reveal giant crustal wedges and transcrustal ramps. Geophys. Res. Lett. 29 (10), doi:10.1029/2002GL014911.

Yliniemi, J., Tiira, T., FIRE WORKING GROUP, 2004. Wide-angle measurements using Vibroseis as the source of the energy during FIRE-project in Finland. Seismix 2004. 11th International Symposium on Deep Structure of the Continents and their Margins, Programme and Abstracts, 26 September–1 October 2004, Centre des congres, Mont-Tremblant, Quebec, Canada.

Yushin, V.I., 1982. On the results of measurements of vibroseismic signals and noise level in vibro-DSS. Sov. Geol. Geophys. 23, 84–88.

Zelt, C.A., Smith, R.B., 1992. Seismic travel time inversion for 2-D crustal velocity structure. Geophys. J. Int. 108, 16–34.

Zelt, C.A., Sain, K., Naumenko, J.V., Sawyer, D.S., 2003. Assessment of crustal velocity models using seismic refraction and reflection tomography. Geophys. J. Int. 153, 609–626.